applied sciences

MDPI

Article

Influence of Pre-Radiation and Photo-Bleaching on the Yb-Doped Fiber Laser Radiated with Gamma-ray

Xuefeng Wang, Shihao Sun *, Ye Zheng *, Miao Yu, Siyuan Li, Yi Cao and Junlong Wang

Beijing Institute of Aerospace Control Devices, Beijing 100094, China; xuefengwang_biacd@163.com (X.W.); yumiao0042@163.com (M.Y.); sdybcao@163.com (Y.C.); wjl_casc@126.com (J.W.)
* Correspondence: sunshihaojob@gmail.com (S.S.); zhengye.no1@163.com (Y.Z.)

Abstract: To improve the radiation resistance of Yb-doped fiber lasers, we investigate the influence of pre-radiation and photo-bleaching on the gamma-radiated laser's performance. When the gamma radiation dose is within 10 krad(Si) with a radiation dose rate less than 0.4 rad(Si)/s, compared to the output power of a non-pre-radiated Yb-doped fiber laser, the pre-radiation technique could enhance the radiation resistance against gamma-ray. However, the mode instability threshold was decreased, which was caused by the cumulated radiation-induced attenuation of pre-radiation and radiation. Based on an electronic probe micro-analyzer, the Yb-doped active fiber was Yb-doped aluminophosphosilicate ternary fiber; therefore, the radiated defects were mainly hole-related defects. A laser diode centered at 532 nm was chosen as the photo-bleaching laser source, which could recover 45.2% of the radiated-induced attenuation and increase the mode instability threshold. This work demonstrates the influence of pre-radiation and photo-bleaching on the radiation resistance against the gamma-ray of Yb-doped fiber lasers, which are of significance in the design and fabrication of related fiber lasers.

Keywords: Yb-doped fiber; fiber laser; gamma radiation; pre-radiation; photo-bleaching

Citation: Wang, X.; Sun, S.; Zheng, Y.; Yu, M.; Li, S.; Cao, Y.; Wang, J. Influence of Pre-Radiation and Photo-Bleaching on the Yb-Doped Fiber Laser Radiated with Gamma-ray. *Appl. Sci.* **2023**, *13*, 6146. https://doi.org/10.3390/app13106146

Academic Editor: John Xiupu Zhang

Received: 17 April 2023
Revised: 15 May 2023
Accepted: 15 May 2023
Published: 18 May 2023

1. Introduction

In recent years, due to the superior characteristics of low quantum defect, the favorable band structure of trivalent Ytterbium (Yb^{3+}) ions, and good beam quality, Yb-doped silica fibers have been considered the ideal amplifying medium for high-power fiber lasers and amplifiers [1–6]. Yb-doped fiber lasers have rapidly expanded their market shares in the commercial laser region and have been widely used in scientific research and industrial processing areas [7–20]. For different working environments, the Yb-doped fiber lasers should be specially designed, such as satisfying the demands of anti-interference and anti-vibration requirements [15]. When operating in an ionizing radiation environment, such as nuclear power plants and radiotherapy facilities, the Yb-doped fiber lasers should be designed with an anti-radiation ability [21–23].

For high-power Yb-doped fiber lasers, which benefited from the tremendous improvement in the material component design and fabrication technology, the output power scale has exponentially increased to tens of kilowatts [11–13]. However, the photodarkening (PD) effect is inevitable for Yb-doped fiber lasers operating at high output power. PD would induce additional absorption in the UV and visible wavelength range with an absorption tail overlap with the pump wavelengths of Yb^{3+}, caused by the formation of defects [24]. When operating in an ionizing radiation environment, the durability of high-power Yb-doped fiber lasers would be faced with more serious challenges [22,23]. Besides the PD effect, high-power Yb-doped fibers would suffer from a more severe output power decrease and the additional absorption, known as the radiation-darkening (RD) effect [22–29]. S. Girard et al. found that the additional absorb intensity of rare-earth-doped fiber is approximately three orders of magnitude higher than that of non-rare-earth-doped passive fibers [22].

Therefore, improving the radiation resistance of high-power Yb-doped fiber lasers is of research and practical significance.

Numerous approaches to improve the radiation resistance of Yb-doped fibers have been proposed, which were mainly separated as the anti-radiation design before ionizing radiation and the bleaching recovery method after ionizing radiation. The material design of Yb-doped fibers to improve the radiation resistance is the most promising approach. For the Yb-doped aluminophosphosilicate ternary fiber, L. Hu et al. discovered that changing the P/Al ratio would influence the degree of RD effect and the kinds of radiation-induced defects [22]. Keeping the elemental concentration of P > Al benefits the radiation resistance and lightens the reduction of Yb^{3+} ions affected by radiation, according to their research. For the Yb/Ce-codoped aluminosilicate binary fiber, N. Dai et al. found that doing $Ce^{3+/4+}$ ions could greatly improve the radiation resistance against gamma-ray of Yb-doped glasses without obvious impact on the absorption properties [29]. However, the negative effects of Yb-doped fibers' material design are not neglectable. When the concentration of P is larger than Al, the absorption and emission cross-section would be decreased, leading to a degradation in the laser performance of Yb-doped ternary fibers [22]. For Yb/Ce-codoped binary fibers, the fluorescence intensity and lifetime of Yb^{3+} ions would be significantly decreased by a high concentration of $Ce^{3+/4+}$ ions [29], and the interaction between Yb^{3+} and $Ce^{3+/4+}$ ions would induce additional thermal load. Therefore, the material design approach still needs abundant experiments and data accumulation. Moreover, pre-radiation and photo-bleaching methods, considered to be key techniques in the relevant research field, are effective and easy to achieve [30–34].

The pre-radiation technique was proven to be quite effective at low output power [30,31]. D.L. Griscom found that extrinsic color centers of pure-silica-core optical fibers were eventually eradicated after a synthetic treatment of ultra-high dose gamma radiation and visible light fluence, and the hardening ability against radiation of this fiber was improved [30]. A. Yeniay demonstrated a method to enhance the radiation hardness of the fibers with respect to induced optical loss by a combined treatment of pre-radiation exposure and thermal annealing, which are applied in a low dose gamma radiation environment, such as in satellite communication systems [31]. The influence of pre-radiation on the radiation resistance of high-power fiber lasers also needs to be further researched. On the other hand, the cumulated radiation-induced attenuation caused by pre-radiation and radiation would contribute to some negative effects at high output power, such as additional thermal load and the mode instability (MI) effect [35–37]. The crucial factor of the photo-bleaching technique is the choosing of bleaching lasers' wavelength, which should be effective enough to bleach the radiation-induced defects, while should not cause additional defects of silica fiber [32–34]. Researching the influence of pre-radiation and photo-bleaching on the radiation resistance against gamma-ray of high output power Yb-doped fiber lasers is urgent and meaningful work.

In this work, we mainly radiated the Yb-doped fiber amplifiers and kept the seed's state steady. With the same gamma radiation dose, the power reduction of pre-radiated fiber laser is approximately 9.80%, less than the 11.10% in the non-radiated fiber laser. Whereas, the cumulated radiation-induced attenuation indeed caused the MI effect, which was observed from the time domain and frequency signal of the output laser. Through the subsequent photo-bleaching process, the output power of pre-radiated fiber laser was further recovered by 80 W, and the MI effect also disappeared. With the radiated Yb-doped fibers bleached to their saturation state, the radiation-induced absorbing intensity at 640 nm approximately decreased by 45.2%. This research is of great significance in the design and fabrication of related fiber lasers or amplifiers against gamma radiation.

2. Experiments

2.1. Laser Setup

In this research, the commercial Yb-doped fiber (Nufern-976-20/400) was used as the active fiber in the fiber laser system. Using gamma-ray radiation at a dose of 5 krad(Si),

the pre-radiated Yb-doped fiber was processed and fabricated into a pre-radiated fiber laser, while the non-pre-radiated fiber laser was fabricated by the Yb-doped fiber without pre-radiation. Except for the active fiber, both fiber lasers had the same configuration, as shown in Figure 1. Output power of the seed laser from the homemade 1060 nm oscillating cavity was about 10 W, with a narrow 3 dB bandwidth of 0.1 nm. The seed laser was followed by a high-power optical isolator (ISO, HPI-1064-20W, provided by Advanced Fiber Resources, Inc.) to isolate backward light and protect the oscillating cavity seed. A mode-field adaptor (MFA, fabricated by Raycuslaser, Inc., Wuhan, China) connected the seed with the amplifier stage, matching the core/cladding size of 10/125 μm in the oscillator stage and 20/250 μm in the combiner's signal fiber. The (6 + 1) × 1 combiner (fabricated by Raycuslaser, Inc., Wuhan, China) injected the seed laser into the active fiber together with the 976 nm amplifier pump light. The pump power of non-pre-radiated and pre-radiated fiber lasers was 1277 W and 1089 W, respectively. The length of both active fibers was 12 m, and a counter-pump (6 + 1) × 1 combiner (fabricated by Raycuslaser, Inc., Wuhan, China) provided the potential ability to further expand the pump power in fiber lasers. A cladding light stripper (CLS, fabricated by Raycuslaser, Inc., Wuhan, China) was used to stripe the residual pump, and a quartz blockhead (QBH, fabricated by Raycuslaser, Inc., Wuhan, China) was spliced to deliver the output laser. The output power was measured with a 10 Kw power meter (10K-W-BB-45, Ophir Inc., Littleton, CO, USA).

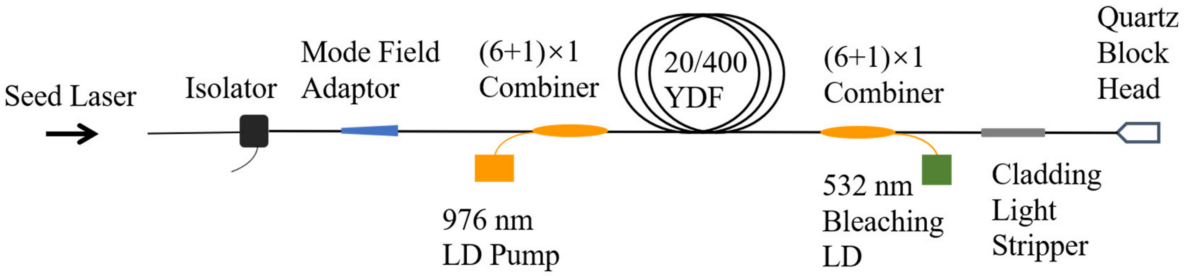

Figure 1. Schematic diagram of the Yb-doped fiber laser system.

2.2. Radiation and Photo-Bleaching Experiment

Both the non-pre-radiated and pre-radiated fiber lasers were radiated with the gamma-ray from a ^{60}Co source of Beijing Normal University in a normal atmosphere at room temperature. The performance of both fiber lasers was researched and recorded when their radiation dose reached 1 krad(Si), 3 krad(Si), and 10 krad(Si), respectively. In the previous two radiation experiments, the dose rate was 0.1 rad(Si)/s, while the dose rate of the last experiment was increased to 0.4 rad(Si)/s to compress the radiation duration. The properties of pre-radiated and non-pre-radiated fiber lasers were contrastively investigated, such as output power, output laser spectra, laser's central wavelength, and 3 dB bandwidth, to research the improvement of pre-radiation on the radiation resistance against gamma-ray.

To identify the crucial doping elements in the fiber core, the radial elemental concentration was researched with an electronic probe micro-analyzer (EPMA). Wavelength of the photo-bleaching laser has a tremendous influence on the bleaching effect of radiated fiber lasers. The 532 nm laser is considered an ideal photo-bleaching laser source, with the ability to convert Yb^{2+} ions into Yb^{3+} ions and simultaneously eliminate hole-related defects such as AlOHC and POHC [34,38]. In this work, 532 nm light from the photo-bleaching LD fabricated by the Institute of Semiconductors (China Academy of Science, Beijing, China) with the maximum power of 6 W was injected from a pump fiber of the counter-pump combiner into the radiated fiber laser to investigate the photo-bleaching effect. Moreover, a 532 nm laser was also injected into the radiated Yb-doped commercial fiber to investigate the variation of absorption spectra.

3. Results and Discussions of Pre-Radiation

3.1. Output Power

Output power reduction is the most obvious radiation-induced effect on fiber lasers. We investigated the linear relationship between output power and pump power of both fiber lasers. We also fitted the linear relationship to compare the slope efficiency at different radiation doses, as shown in Figure 2. The linear relationship was presented by the dotted lines, and output power with its error bar was also demonstrated with the hollow symbols in Figure 2. For the non-pre-radiated fiber laser with 0 krad(Si), the output power was about 1065 W with a slope efficiency of 82.6%, as shown in Figure 2a. When the cumulated radiation dose reached 1 krad(Si) and 3 krad(Si) with a dose rate of 0.1 rad(Si)/s, output power of the non-pre-radiated fiber laser hardly decreased, with the corresponding slope efficiency of 83.2% and 82.0%, respectively. When the radiation dose rate increased to 0.4 rad(Si)/s and the cumulated radiation dose reached 10 krad(Si), the output power rapidly decreased to 946 W with a slope efficiency of 74.1%.

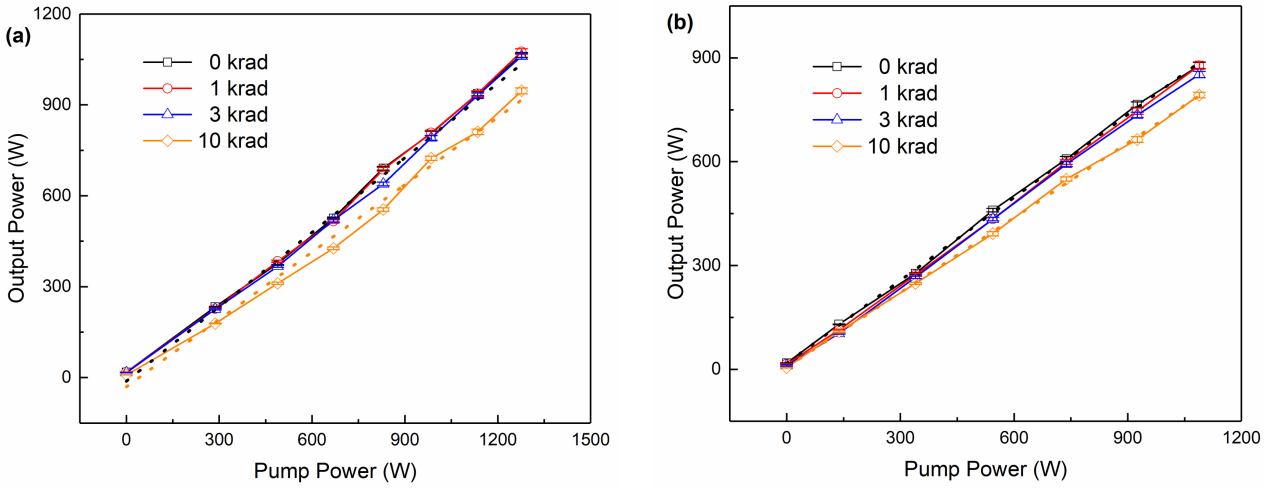

Figure 2. Output power of fiber lasers at different radiation doses, (**a**) the non-pre-radiated fiber laser, (**b**) the pre-radiated fiber laser, hollow symbols for the output power and the corresponding error bars, black dotted lines for the fitted linear relationship of 0 krad, yellow dotted lines for the fitted linear relationship of 10 krad.

For the pre-radiated fiber laser with 0 krad(Si), the output power was approximately 878 W with a slope efficiency of 79.8%. When the cumulated radiation dose reached 1 krad(Si) and 3 krad(Si), the output power was slightly decreased, with the corresponding slope efficiency of 79.8% and 78.6%, respectively. When the cumulated radiation dose reached 10 krad(Si) with the rate of 0.4 rad(Si)/s, the output power decreased to 792 W with a slope efficiency of 72.1%, as shown in Figure 2b.

The output power performance at different cumulated radiation doses was shown in Figure 3. When the cumulated radiation reached 10 krad(Si), the output power of the non-pre-radiated fiber laser decreased to 88.8% with the reduction of 119 W, while the pre-radiated fiber laser decreased to 90.2% with the reduction of 86 W. Compared to the non-pre-radiated fiber laser, the output power of the pre-radiated fiber laser was less reduced, which presented a higher radiation resistance. Whereas, the mode instability effect was observed in the pre-radiated fiber laser, caused by the cumulated radiation-induced attenuation of pre-radiation and radiation.

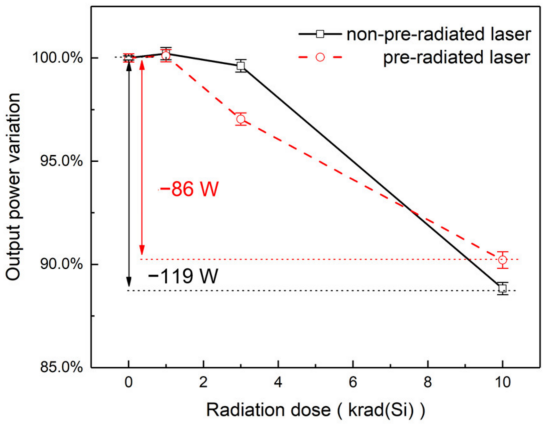

Figure 3. Output power of fiber lasers at different radiation doses, black solid line for the non-pre-radiated fiber laser, red dashed line for the pre-radiated fiber laser, hollow symbols for the output power variation, and the corresponding error bars.

When the cumulated radiation dose reached 10 krad(Si) and pump power reached the maximum, the output power of the pre-radiated fiber laser presented fluctuation. Measured with a highspeed Si Biased photodetector (DET02AFC, provided by Thorlabs Inc., Newton, NJ, USA) with a detection range of 400~1100 nm and a mixed domain oscilloscope (MDO3054, provided by Tektronix Inc., Beaverton, OR, USA) with a sampling rate of 2.5 GS/s, the time domain and frequency signals of the output laser were analyzed, as shown in Figure 4. The voltage fluctuation could be observed on the millisecond scale in the time domain, and peaks around 5 kHz could also be recognized in the frequency domain. From the time and frequency domain analysis, the mode instability effect of the pre-radiated fiber laser in this state could be confirmed [36,37]. When the output power of a fiber laser exceeds a certain threshold power, the mode instability effect occurs when the output laser's mode changed from a stable fundamental mode to an unstable mode. The energy between different modes is dynamically coupled at a millisecond scale, resulting in sudden degradation of the directionality and beam quality of the output beam. The time domain characteristics of typical mode instability effects exhibit periodicity at a millisecond scale, and the frequency domain exhibits a coupling frequency on the kHz level, consistent with the results in Figure 4.

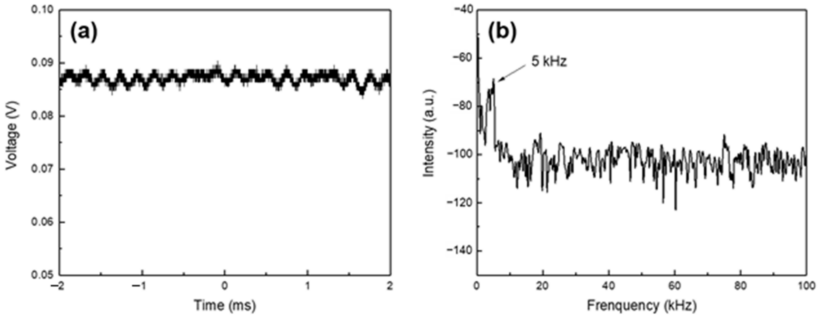

Figure 4. (**a**) Time domain and (**b**) frequency domain properties of the output laser in pre-radiated fiber laser.

3.2. Spectral Properties

Besides the output power reduction, radiation would also influence the spectral properties of the output laser. We measured the output laser's spectra at different output powers pumped by a 976 nm LD and with different radiation doses per the Telecom Optical Spectrum Analyzer (OSA, AQ6370D, from Yokogawa Inc., Musashino City, Japan). Figure 5a presents the output laser spectrum at 946 W of the non-pre-radiated fiber laser with 10 krad(Si) radiation. The central wavelength is 1060.25 nm with a narrow 3 dB band-

width of 0.1258 nm, and the suppression ratio reached 30.0 dB between the signal peak and the Stimulated Raman Scattering (SRS) peak centered at 1113 nm. As a kind of non-linear effect, the intensity of the SRS peak is related to the fiber length and output power. The insert of Figure 5a is the signal peak with a narrow wavelength range. Figure 5b presents the output laser spectrum at 792 W of the pre-radiated fiber laser with 10 krad(Si) radiation, showing the same central wavelength with a narrow 3 dB bandwidth of 0.1258 nm. The SRS suppression ratio was also 30.0 dB. With the same radiation dose, pre-radiation treatment has little influence on the spectral property of radiated fiber lasers.

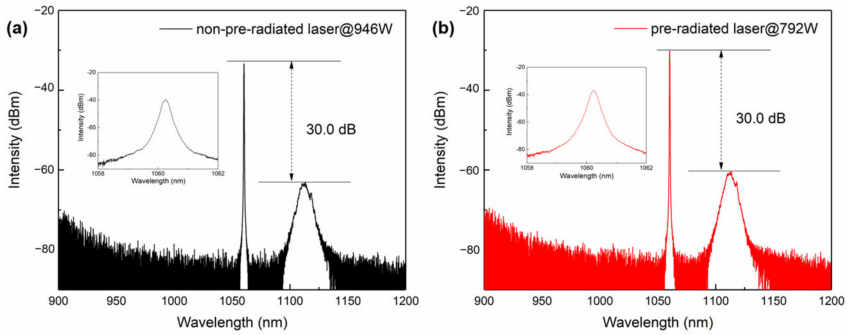

Figure 5. The output laser spectra of (**a**) non-pre-radiated fiber laser radiated by 10 krad(Si), (**b**) pre-radiated fiber laser radiated by 10 krad(Si), inserts present the laser spectra within a narrow wavelength range.

The spectral properties at different cumulated radiation doses were measured, as shown in Figure 6. The central wavelength of both fiber lasers slightly fluctuated within the range between 1060.22 nm and 1060.26 nm. Due to the seed laser not being radiated with gamma ray, the fluctuation mainly originated from a testing error or a tiny change in environmental conditions. With the radiation cumulated, 3 dB bandwidth of the non-pre-radiated fiber laser slightly decreased from 0.1450 nm to 0.1258 nm, and 3 dB bandwidth of the pre-radiated fiber laser decreased from 0.1481 nm to 0.1258 nm. The SRS suppression ratio also changed, within the range of 28.9 dB to 31.4 dB. Considering the measuring accuracy of the spectrograph and the experimental error during the test, it can be concluded that the radiation dose at this level has little influence on the spectral properties, such as the central wavelength, 3 dB bandwidth, and SRS suppression ratio.

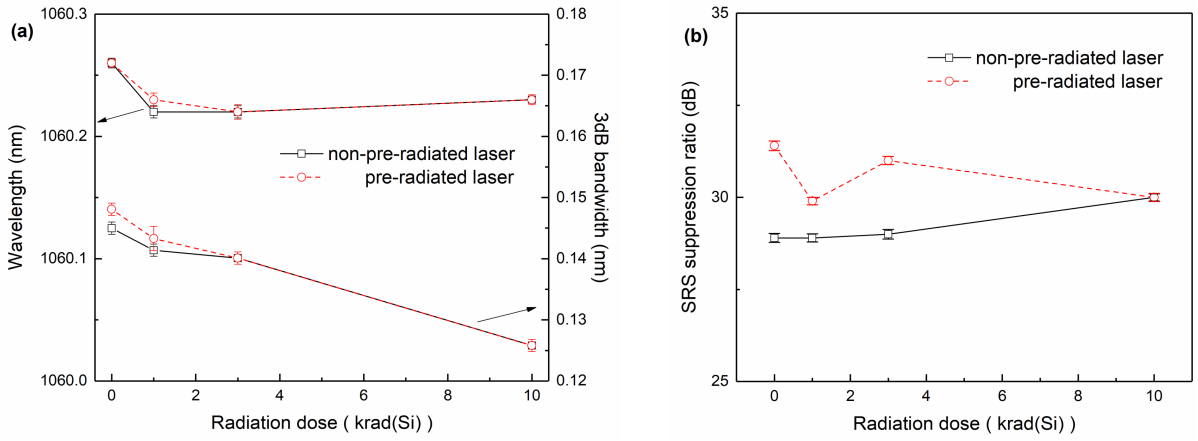

Figure 6. Spectral properties of fiber lasers at different radiation doses, (**a**) the central wavelength and 3 dB bandwidth of the output laser (arrows represent the coordinate axis corresponding to the lines), (**b**) the SRS suppression ratio of the output laser.

In summary, within the current radiation dose range (less than 10 krad), the main influence mechanism of radiation on fiber lasers is the radiation-induced attenuation effect.

The obvious output power reduction can be observed, while there is no significant change in spectral properties. When the gamma radiation dose is within 10 krad, pre-radiation treatment can slightly strengthen the radiation resistance of high-power fiber lasers against gamma-ray, as proven in Figure 3. The reason pre-radiation enhances the radiation resistance of Yb-doped fibers is partly related to the increasing OH, which originated from the reaction of H^+ ions from the fibers' coating layer radiated with gamma-ray and the intrinsic SiO_2 units in fiber [38–40]. Whereas, the mode instability threshold would decrease at high-power output states, due to the cumulated radiation-induced attenuation of pre-radiation and radiation, which needs to be comprehensively considered before the pre-radiation treatment is implemented.

4. Results and Discussions of Photo-Bleaching

4.1. Output Power

In material science, it is usually necessary to study and observe the morphology and chemical composition of samples at the micrometer scale. Radiation resistance of Yb-doped fibers is closely related to the fibers' doping elements. The type of commercial Yb-doped fiber in this research is Nufern-976-20/400, presenting a stronger radiation resistance than the Yb-doped aluminophosphosilicate ternary fiber in our previous work [41]. Therefore, an EPMA was applied to identify the crucial doping elements in this commercial Yb-doped fiber core. EPMA is a relatively mature testing instrument, which uses an electron beam to excite the intersecting surface of Yb-doped fiber samples and perform feature analysis on various signals generated. Carbon needs to be sprayed on the intersecting surface of fiber samples to make it conductive.

The radial elemental concentration of Al_2O_3, P_2O_5, and Yb_2O_3 was measured to be 1.13 mol%, 2.20 mol%, and 0.15 mol%, respectively, as shown in Figure 7. With the molar ratio of (Al + P)/Yb being more than 22:1, Yb ions could be sufficiently dissolved in the fiber core area, which would prevent Yb ions from clustering and increase the fluorescence lifetime [42–44]. The concentration of P is approximately twice that of Al, which is helpful to improve the radiation resistance, due to the formation of $[AlPO_4]$ units with a large charge-compensating effect, and excess P formed a solvation shell surrounding Yb^{3+} ions [22].

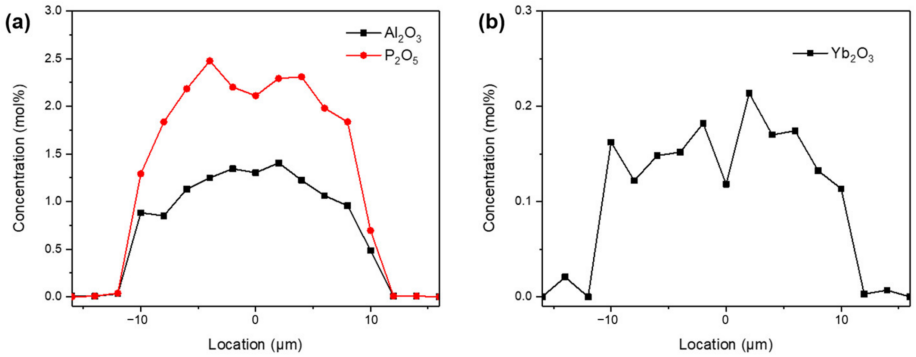

Figure 7. Radial elemental concentration profiles in the Yb-doped commercial fiber core, (**a**) Al_2O_3 and P_2O_5, (**b**) Yb_2O_3.

Due to the ability to convert Yb^{2+} ions into Yb^{3+} ions and simultaneously eliminate the hole-related defect [34,38], the 532 nm laser was suitable as a photo-bleaching source for the radiated Yb_2O_3-Al_2O_3-P_2O_5 ternary fiber. To investigate the bleaching effect, 532 nm light was fed into the pre-radiated fiber laser with 10 krad(Si) radiation, as shown in Figure 8a. The power of 532 nm light was 5 W, and the photo-bleaching duration lasted 2 h. After the bleaching treatment, we measured the output power of the fiber laser, as shown in Figure 8b. The output power of the pre-radiated fiber laser partly recovered with an increase of 26 W, and the slope efficiency also recovered to 74.8%. The research indicated that part of the radiation-induced defect was bleached by 532 nm light, and the output

power has been correspondingly increased while the radiation-induced thermal load partly decreased. Time and frequency domain signals of the output laser were also investigated by the combination of the above-mentioned highspeed photodetector and oscilloscope, which proved no MI effect existed at this pump power. In this research, the MI threshold raised approximately 227 W through the photo-bleaching treatment of 532 nm light.

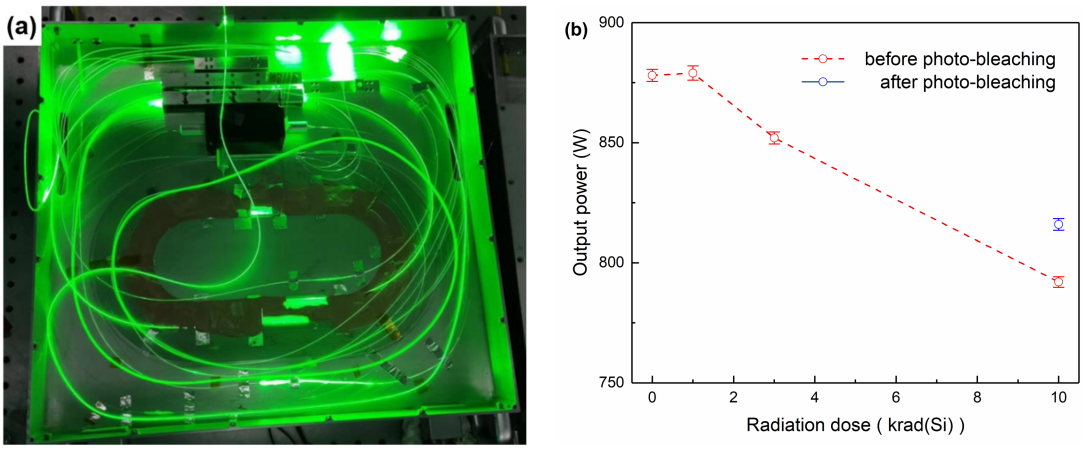

Figure 8. Photo-bleaching treatment of the pre-radiated fiber laser with 10 krad radiation, (**a**) experimental setup, (**b**) output power performance, hollow symbols for the output power and the corresponding error bars.

4.2. Spectral Properties

To further investigate the photo-bleaching mechanism, the absorption spectra of a radiated Yb-doped fiber were measured. The 13 m long Yb-doped fiber was radiated with 7 krad(Si) gamma-ray, and the radiated Yb-doped fiber was subjected to multiple accumulated photo-bleaching treatments. The absorption spectra of this fiber at different states were recorded in Figure 9. Before radiation, the pristine fiber demonstrated a typical absorption spectrum of Yb-doped fiber with a broadband absorption at 915 nm and an intense absorption at 976 nm. After radiation, a broad radiation-induced absorption centered at 640 nm could be observed. With the injection of photo-bleaching laser, the absorption intensity at 640 nm gradually decreased, meaning part of the radiation-induced defect was bleached by the 532 nm laser. After a total photo-bleaching treatment of 7.25 h at 1.5 W and 4 h at 5 W, the absorption intensity at 640 nm no longer changed. The radiation-induced absorption had been bleached to its saturation state.

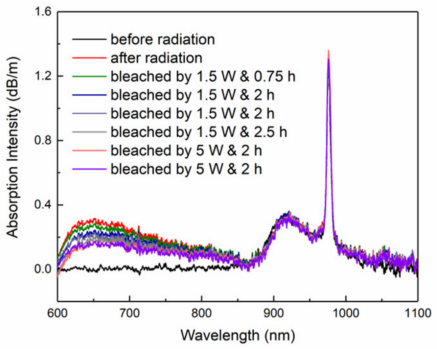

Figure 9. Absorption spectra of radiated Yb-doped fiber with 7 krad radiation photo-bleached by injecting different bleaching lasers.

A quantitative relationship between the photo-bleaching energy and radiation-induced attenuation at 640 nm was investigated, as shown in Figure 10a. After radiation, the absorption intensity at 640 nm rapidly increased to 0.32 dB/m, caused by the formation

of radiation-induced defects in the fiber core. With the augment of bleaching energy at 532 nm injected, the absorption intensity at 640 nm gradually decreased originating from a gradual reduction of gamma-radiation-induced defects by the bleaching effect of the 532 nm laser. Finally, the loss at 640 nm reached its saturation, and approximately 45.2% of radiation-induced absorption could be bleached with the 532 nm laser. The bleaching efficiency (absorption intensity bleached per 532 nm energy) after different bleaching treatments was plotted in Figure 10b. Generally, the bleaching efficiency gradually decreased with the gradual reduction of gamma-radiation-induced defects from the bleaching effect, and, finally, it was close to 0 at the saturation state.

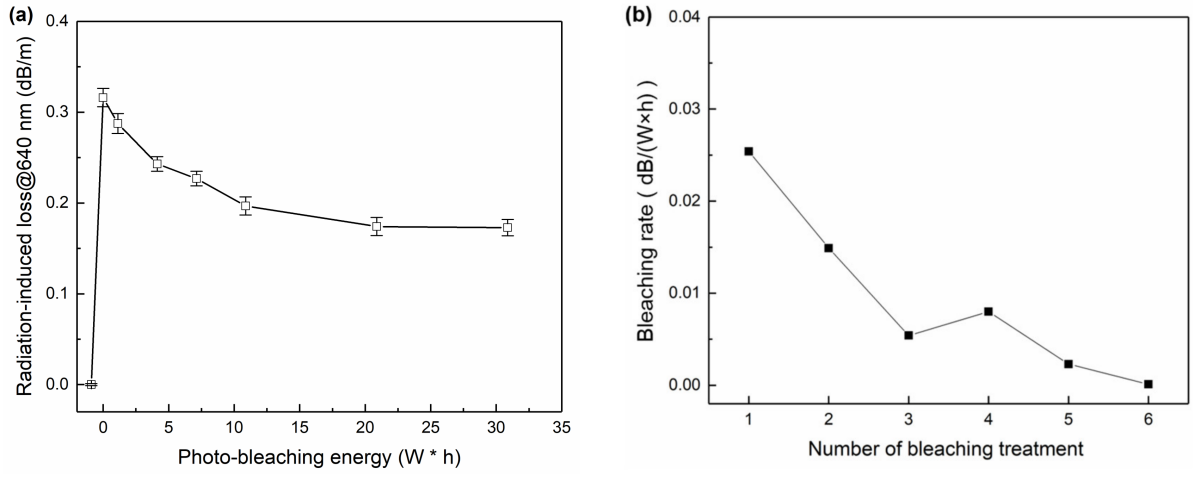

Figure 10. Quantitative research of photo-bleaching effect, (**a**) absorption intensity at 640 nm versus photo-bleaching energy, (**b**) bleaching efficiency versus the number of bleaching treatments.

In summary, a laser diode at 532 nm was applied to bleach the radiated fiber laser and radiated Yb-doped fiber. The output power of the fiber laser partly recovered by 26 W, and the corresponding slope efficiency also recovered from 72.1% to 74.8%. The simultaneous reduction of radiation-induced attenuation from the photo-bleaching treatment also leads to an improvement in the MI threshold. In this work, approximately 45.2% of radiation-induced absorption could be bleached by the 532 nm laser, reaching the bleaching saturation state. The quantitative relationship between the photo-bleaching energy and radiation-induced absorption at 640 nm was also investigated.

5. Conclusions

To improve the radiation resistance of high-power Yb-doped fiber lasers, the influence of pre-radiation and photo-bleaching on the gamma-radiated laser's performance was researched in this work. The pre-radiated fiber laser and non-pre-radiated fiber laser were fabricated with the pre-radiated Yb-doped fiber and pristine Yb-doped fiber, respectively. Except for the active fiber, both fiber lasers had the same configuration. The laser performance of non-pre-radiated and pre-radiated fiber lasers after gamma radiation was comparatively investigated. When the gamma radiation dose is within 10 krad(Si) with the radiation dose rate of less than 0.4 rad(Si)/s, pre-radiation treatments would improve the radiation resistance against gamma-ray to a certain extent, showing less output power reduction. However, the mode instability threshold would be decreased, due to the cumulated radiation-induced attenuation caused by pre-radiation and radiation. Therefore, the radiation induced MI effect in high-power fiber lasers needs to be comprehensively considered before the pre-radiation treatment is implemented.

Considering the doping element of this commercial Yb-doped fiber, a laser diode at 532 nm was applied as the photo-bleaching laser source. In this research, the output power of the fiber laser partly recovered by 26 W, and the slope efficiency also recovered from 72.1% to 74.8%. The MI threshold was also increased. According to the research on

bleaching treatment of the radiated Yb-doped fiber, approximately 45.2% radiated-induced attenuation was bleached by the 532 nm laser, reaching the bleaching saturation state. This research is of significance in the design and fabrication of high-power fiber lasers against gamma radiation.

Author Contributions: Investigation, M.Y. and S.L.; Resources, Y.C.; Writing—original draft, S.S.; Writing—review & editing, Y.Z.; Project administration, J.W.; Funding acquisition, X.W. All authors have read and agreed to the published version of the manuscript.

Funding: This work was supported by the National Natural Science Foundation of China (No. U20B2058).

Institutional Review Board Statement: Not applicable.

Informed Consent Statement: Not applicable.

Data Availability Statement: The data presented in this study are available from the corresponding author, upon reasonable request. The data are not publicly available due to privacy.

Conflicts of Interest: The authors declare no conflict of interest.

References

1. Jauregui, C.; Limpert, J.; Tünnermann, A. High-power fibre lasers. *Nat. Photonics* **2013**, *7*, 861–867. [CrossRef]
2. Zhou, P.; Wang, X.; Xiao, H.; Ma, Y.; Chen, J. Review on recent progress on Yb-doped fiber laser in a variety of oscillation spectral ranges. *Laser Phys.* **2012**, *22*, 823–831. [CrossRef]
3. Hideur, A.; Chartier, T.; Özkul, C.; Sanchez, F. Dynamics and stabilization of a high power side-pumped Yb-doped double-clad fiber laser. *Opt. Commun.* **2000**, *186*, 311–317. [CrossRef]
4. Hecht, J. A short history of laser development. *Appl. Opt.* **2010**, *49*, F99–F122. [CrossRef] [PubMed]
5. Zheng, Y.; Zhu, Z.; Liu, X.; Yu, M.; Li, S.; Zhang, L.; Ni, Q.; Wang, J.; Wang, X. High-power, high-beam-quality spectral beam combination of six narrow-linewidth fiber amplifiers with two transmission diffraction gratings. *Appl. Opt.* **2019**, *58*, 8339–8343. [CrossRef] [PubMed]
6. Zheng, Y.; He, M.; Liu, X.; Ma, Z.; Chen, J.; Yu, M.; Li, S.; Cao, Y.; Wang, J.; Wang, X. Experimental Study on High-Power Laser Beam Combining Using Dichroic Mirrors. *Laser Optoelectron. Prog.* **2023**, *60*, 1514002.
7. Deschamps, T.; Ollier, N.; Vezin, H. Gonnet, Clusters dissolution of Yb^{3+} in codoped SiO_2-Al_2O_3-P_2O_5 glass fiber and its relevance to photodarkening. *J. Chem. Phys.* **2012**, *136*, 014503. [CrossRef] [PubMed]
8. Peng, K.; Wang, Y.; Ni, L.; Wang, Z.; Gao, C.; Zhan, H.; Wang, J.; Jing, F.; Lin, A. Yb-doped large-mode-area laser fiber fabricated by hal-ide-gas-phase-doping technique. *Laser Phys.* **2015**, *25*, 065801. [CrossRef]
9. Richardson, D.J.; Nilsson, J.; Clarkson, W.A. High power fiber lasers: Current status and future perspectives. *J. Opt. Soc. Am. B* **2010**, *27*, B63–B92. [CrossRef]
10. Zervas, M.N.; Codemard, C.A. High Power Fiber Lasers: A Review. *IEEE J. Sel. Top. Quantum* **2014**, *20*, 219–241. [CrossRef]
11. Jeong, Y.; Sahu, J.K.; Payne, D.N.; Nilsson, J. Ytterbium-doped large-core fiber laser with 1.36 kW continuous-wave output power. *Opt. Express* **2004**, *12*, 6088–6092. [CrossRef] [PubMed]
12. Fang, Q.; Shi, W.; Qin, Y.; Meng, X.; Zhang, Q. 2.5 kW monolithic continuous wave (CW) near diffraction-limited fiber laser at 1080 nm. *Laser Phys. Lett.* **2014**, *11*, 105102. [CrossRef]
13. Shcherbakov, E.A.; Fomin, V.V.; Abramov, A.A.; Ferin, A.A.; Mochalov, D.V.; Gapontsev, V.P. Industrial grade 100 kW power CW fiber laser. In *Advanced Solid-State Lasers*; Optical Society of America: Washington, DC, USA, 2013; p. ATh4A.2.
14. Zheng, Y.; Ni, Q.; Zhang, L.; Liu, X.; Wang, J.; Wang, X. Influence of Stimulated Raman Scattering on Propagation Properties of High-Power Laser. *Chin. J. Lasers* **2021**, *48*, 0701005. [CrossRef]
15. Zheng, Y.; Liu, X.; He, M.; Zhang, L.; Yu, M.; Li, S.; Ma, Z.; Wang, J.; Wang, X. Investigation on the thermal blooming effect in a high power spectral beam combining fiber laser system. *Appl. Opt.* **2022**, *61*, 954–959. [CrossRef] [PubMed]
16. Wan, Y.; Wen, J.; Jiang, C.; Tang, F.; Wen, J.; Huang, S.; Pang, F.; Wang, T. Over 255 mW single-frequency fiber laser with high slope efficiency and power stability based on an ultrashort Yb-doped crystal-derived silica fiber. *Photonics Res.* **2021**, *9*, 649–656. [CrossRef]
17. Zhao, Z.; Jin, L.; Set, S.Y.; Yamashita, S. Broadband similariton generation in a mode-locked Yb-doped fiber laser. *Opt. Lett.* **2022**, *47*, 2238–2241. [CrossRef]
18. Ye, Y.; Lin, X.; Yang, B.; Xi, X.; Shi, C.; Zhang, H.; Wang, X.; Li, J.; Xu, X. Tapered Yb-doped fiber enabled a 4 kW near-single-mode monolithic fiber amplifier. *Opt. Lett.* **2022**, *47*, 2162–2165. [CrossRef]
19. Beetar, J.E.; Nrisimhamurty, M.; Truong, T.-C.; Liu, Y.; Chini, M. Thermal effects in molecular gas-filled hollow-core fibers. *Opt. Lett.* **2021**, *46*, 2437–2440. [CrossRef]
20. Wang, W.; Wu, H.; Liu, C.; Sun, B.; Liang, H. Multigigawatt 50 fs Yb: CALGO regenerative amplifier system with 11 W average power and mid-infrared genera-tion. *Photonics Res.* **2021**, *9*, 1439–1445. [CrossRef]

21. Girard, S.; Ouerdane, Y.; Tortech, B.; Marcandella, C.; Robin, T.; Cadier, B.; Baggio, J.; Paillet, P.; Ferlet-Cavrois, V.; Boukenter, A.; et al. Radiation Effects on Ytterbium- and Ytterbium/Erbium-Doped Double-Clad Optical Fibers. *IEEE Trans. Nucl. Sci.* **2009**, *56*, 3293–3299. [CrossRef]
22. Shao, C.; Ren, J.; Wang, F.; Ollier, N.; Xie, F.; Zhang, X.; Zhang, L.; Yu, C.; Hu, L. Origin of radiation-induced darkening in $Yb^{3+}/Al^{3+}/P^{5+}$-doped silica glasses: Effect of the P/Al ratio. *J. Phys. Chem.* **2018**, *B122*, 2809–2820. [CrossRef] [PubMed]
23. Duchez, J.-B.; Mady, F.; Mebrouk, Y.; Ollier, N.; Benabdesselam, M. Interplay between photo- and radiation-induced darkening in ytterbium-doped fibers. *Opt. Lett.* **2014**, *39*, 5969–5972. [CrossRef] [PubMed]
24. Deschamps, T.; Vezin, H.; Gonnet, C.; Ollier, N. Evidence of AlOHC responsible for the radiation-induced darkening in Yb doped fiber. *Opt. Express* **2013**, *21*, 8382–8392. [CrossRef] [PubMed]
25. Jetschke, S.; Unger, S.; Schwuchow, A.; Leich, M.; Jäger, M. Role of Ce in Yb/Al laser fibers: Prevention of photodarkening and thermal effects. *Opt. Express* **2016**, *24*, 13009–13022. [CrossRef]
26. Berghmans, F.; Brichard, B.; Fernandez, A.F.; Gusarov, A.; Van Uffelen, M.; Girard, S. An Introduction to Radiation Effects on Optical Components and Fiber Optic Sensors. In *Optical Waveguide Sensing and Imaging*; Springer: Berlin/Heidelberg, Germany, 2008; pp. 127–165.
27. Fox, B.P.; Schneider, Z.V.; Simmons-Potter, K.; Thomes, W.J.; Meister, D.C.; Bambha, R.P.; Kliner, D.A.V. Spectrally Resolved Transmission Loss in Gamma Irradiated Yb-Doped Optical Fibers. *IEEE J. Quantum Electron.* **2008**, *44*, 581–586. [CrossRef]
28. Taylor, E.W.; Liu, J. Ytterbium-doped fiber laser behavior in a gamma-ray environment. In *Photonics for Space Environments*; SPIE: Bellingham WA, USA, 2005; p. 58970E. [CrossRef]
29. Sheng, Y.; Yang, L.; Luan, H.; Liu, Z.; Yu, Y.; Li, J.; Dai, N. Improvement of radiation resistance by introducing CeO_2 in Yb-doped silicate glasses. *J. Nucl. Mater.* **2012**, *427*, 58–61. [CrossRef]
30. Griscom, D. Radiation hardening of pure-silica-core optical fibers by ultra-high-dose γ-ray pre-irradiation. *J. Appl. Phys.* **1995**, *77*, 5008–5013. [CrossRef]
31. Yeniay, A.; Gao, R. Radiation induced loss properties and hardness enhancement technique for ErYb doped fibers for avionic applications. *Opt. Fiber Technol.* **2013**, *19*, 88–92. [CrossRef]
32. Friebele, E.J.; Gingerich, M.E. Photobleaching effects in optical fiber waveguides. *Appl. Opt.* **1981**, *20*, 3448–3452. [CrossRef]
33. Manek-Hönninger, I.; Boullet, J.; Cardinal, T.; Guillen, F.; Ermeneux, S.; Podgorski, M.; Doua, R.B.; Salin, F. Photodarkening and photobleaching of an ytterbium-doped silica double-clad LMA fiber. *Opt. Express* **2007**, *15*, 1606–1611. [CrossRef]
34. Guzman Chavez, A.D.; Kir'Yanov, A.V.; Barmenkov, Y.O.; Il'Ichev, N.N. Reversible photo-darkening and resonant photobleaching of Ytterbium-doped silica fiber at in-core 977-nm and 543-nm irradiation. *Laser Phys. Lett.* **2007**, *4*, 734–739. [CrossRef]
35. Smith, A.V.; Jesse, J.S. Mode instability in high power fiber amplifiers. *Opt. Express* **2011**, *19*, 10180–10192. [CrossRef] [PubMed]
36. Tao, R.; Zhou, P.; Xiao, H. Progress of study on mode instability in high power fiber amplifiers. *Laser Optoelectron. Prog.* **2014**, *51*, 020001.
37. Shi, C.; Tao, R.; Wang, X. New progress and phenomena of modal instability in fiber lasers. *Chin. J. Lasers* **2017**, *44*, 0201004.
38. Cao, R.; Lin, X.; Chen, Y.; Cheng, Y.; Wang, Y.; Xing, Y.; Li, H.; Yang, L.; Chen, G.; Li, J. 532 nm pump induced photo-darkening inhibition and photo-bleaching in high power Yb-doped fiber amplifiers. *Opt. Express* **2019**, *27*, 26523–26531. [CrossRef]
39. Brichard, B.; Fernandez, A.F.; Berghmans, F.; Decreton, M. Origin of the radiation-induced OH vibration band in polymer-coated optical fibers irradiated in a nuclear fission reactor. *IEEE Trans. Nucl. Sci.* **2002**, *49*, 2852–2856. [CrossRef]
40. Liu, S.L.S.; Zheng, S.Z.S.; Yang, K.Y.K.; Chen, D.C.D. Radiation-induced change of OH content in Yb-doped silica glass. *Chin. Opt. Lett.* **2015**, *13*, 060602. [CrossRef]
41. Sun, S.; Zhang, L.; Dai, J.; Gao, C.; Li, Y.; Liu, N.; He, H.; Shen, C.; Jiang, L.; Li, F.; et al. Comparative study of γ-radiation resistance between Yb/Ce/F and Yb/P doped aluminosilicate fibers. *Optik* **2021**, *250*, 168347. [CrossRef]
42. Arai, T.; Ichii, K.; Tanigawa, S.; Fujimaki, M. Gamma-radiation-induced photodarkening in ytterbium-doped silica glasses. In *Fiber Lasers VIII: Technology, Systems, and Applications*; SPIE: Bellingham WA, USA, 2011; p. 79140K. [CrossRef]
43. Liu, S.; Zhan, H.; Peng, K.; Li, Y.; Sun, S.; Jiang, J.; Ni, L.; Wang, X.; Yu, J.; Jiang, L.; et al. Multi-kW Yb-doped alumino-phosphosilicate fiber. *Opt. Mater. Express* **2018**, *8*, 2114–2124. [CrossRef]
44. Li, Y.; Peng, K.; Zhan, H.; Liu, S.; Ni, L.; Wang, Y.; Yu, J.; Wang, X.; Wang, J.; Jing, F.; et al. Yb-doped aluminophosphosilicate ternary fiber with high efficiency and excellent laser stability. *Opt. Fiber Technol.* **2018**, *41*, 7–11. [CrossRef]